Local measurement on oedometric compression tests: Time and temperature ageing effects on a fluorosilicone

Clémence Logeais, Cristian Ovalle, Lucien Laiarinandrasana

Mechanics of Materials 200 (2025) 105193

Contents lists available at ScienceDirect

Mechanics of Materials

journal homepage: www.elsevier.com/locate/mecmat

Research paper

Local measurement on oedometric compression tests: Time and temperature ageing effects on a fluorosilicone

Clémence Logeais *, Cristian Ovalle, Lucien Laiarinandrasana

Mines Paris, PSL University, Centre for Material Sciences (MAT), CNRS 7633 BP 87, 63-65 rue Henri Auguste Desbrueres, Corbeil-Essonnes, 91100, France

ARTICLE INFO

Keywords:
Elastomer
Bulk modulus
Ageing
Confined compression

ABSTRACT

O-ring durability is a key issue for engineering structures that require sealing over a long service life. Rubber-like materials are used for this type of component because of the assumption of incompressibility, i.e. a high bulk modulus K. However, this assumption has been called into question in the literature, particularly for elastomers under high hydrostatic pressures. This work examines the compressibility of rubber-like materials, with a particular focus on fluorosilicone elastomers (FVMQ). A method of confined compression using a transparent crucible is presented which allows local measurement of the displacement field. This technique provides a better understanding of the analysis of oedometric compression data and a reliable way to determine the K value. Furthermore, this approach allows following the evolution of K over time with accelerated ageing. Three ageing temperatures – 200, 220 and 250 °C – were tested up to 34, 15 and 1 weeks, respectively. For the three ageing temperatures, the FVMQ results show a decrease in K values with ageing. In particular, at 250 °C, a turning point was observed after 72 h of ageing. These results highlight the influence of ageing on the compressibility of the FVMQ and the presence of two different ageing mechanisms affecting the K evolution.

1. Introduction

Fluorosilicone (FVMQ)[1] elastomer is used in various industrial sectors (Bhuvaneswari et al., 2017) thanks to its exceptional performance in aggressive environments. In particular, it is widely used in sealing systems where durability is critical to ensure reliable operation over a long service life. Sealing quality involves a low volume variation of the material under high hydrostatic pressure, i.e. a high bulk modulus K. Indeed, in this kind of application the elastomer is confined within the edges of its housing. The incompressible character of the elastomers is then a key concept for their sealing ability. However, incompressibility means a bulk modulus tending to infinity. Nevertheless, the assumption of incompressibility is an approximation that does not apply to all elastomers or loading conditions. Some elastomers can exhibit significant volume changes, often referred to as quasi-incompressibility. The bulk modulus is an important parameter for materials under hydrostatic pressure (Zimmermann and Stommel, 2013), laminated rubber (Bouaziz et al., 2020; Hao et al., 2024), and in cavitation failure contexts (Gent and Lindley, 1959; Barney et al., 2020).

To ensure sealing, measuring K becomes an important issue and a great challenge. Two approaches qualified as indirect and direct can be considered. In the indirect approach, determining the bulk modulus consists of deducing it from the Young's modulus E and the Poisson's ratio ν once these material parameters were evaluated. E and ν can be obtained by using various techniques such as dilatometry (Laufer et al., 1978; Farris, 1964; Shuttleworth, 1968; Green, 1921), digital image correlation (DIC) (Xu and Juang, 2021; Farfán-Cabrera et al., 2017; Pritchard et al., 2013) or strain gauges (Smith et al., 1972; Ren et al., 2008). However, measuring ν poses a great challenge in the calculation of K, as reported by Burns et al. (1990) and Burns et al. (1987). Besides, even a minor error in ν can introduce significant uncertainty in the determination of K. The direct approach involves experimental setup of two types of test. The first consists of applying hydrostatic pressure to a material by immersing the specimen in a confining fluid (Weir, 1953; Adams and Gibson, 1930; Scott, 1935; Copeland, 1948; Tizard et al., 2012; Stanojevic and Lewis, 1983), but this method could be difficult to set up because it requires special equipment. Furthermore, the permeability of the material could return an erroneous measure. The second is to apply hydrostatic pressure by enclosing the material in a crucible (Bouaziz et al., 2020; Stanojevic and Lewis, 1983; Holownia, 1975; Tizard et al., 2012). While setting up this method is straightforward, it may introduce challenges in accurately capturing the

* Corresponding author.
E-mail address: clemence.logeais@minesparis.psl.eu (C. Logeais).

[1] Fluoro-vinyl-methyl-siloxane (G-group [ISO 1629]).

https://doi.org/10.1016/j.mechmat.2024.105193
Received 18 April 2024; Received in revised form 5 October 2024; Accepted 4 November 2024
Available online 13 November 2024

mechanical response of the material due to the blind nature of the test. Issues such as stiffness problems could prove challenging to rectify.

Concerning the long-service life, current literature shows a limited understanding of the precise degradation mechanisms associated with FVMQ. In fact, as a modified silicone, the monomeric repeating units of fluorosilicone elastomer exhibit different reactivities compared to conventional silicones, which limits the applicability of existing knowledge on silicones (Camino et al., 2001). While some information is available about their thermal stability and thermal degradation (Cox et al., 1964a,b; Kalfayan et al., 1975; Pires et al., 2022; Thomas, 1972), a full understanding of their mechanical properties, particularly in terms of compressibility, remains limited or even non-existent. Indeed, to the author's knowledge, few papers have been dedicated in the literature, to the experimental determination of the bulk modulus of elastomers (Burns et al., 1990, 1987; Adams and Gibson, 1930; Diani et al., 2008; Barney et al., 2022; Kelly and Lai, 2011; Tabor, 1994; Van Engelen and Kelly, 2015; Zimmermann and Stommel, 2013), less publication were found to investigate the influence of ageing on K. Although, studies have been carried out on the ageing of seals (Bernstein and Gillen, 2009; Cassenti and Staroselsky, 2017; Kömmling et al., 2017), understanding the evolution-on-time of the compressibility of the sealing material is essential to ensure the performance of the seal. Bouaziz et al. (2020) showed the evolution of K over ageing time and temperature for unfilled and filled neoprene. The observations have shown that, measuring the bulk modulus K is a complex task that can introduce significant uncertainties. It is therefore imperative to develop a reliable and accurate method for studying the evolution of compressibility in this material over ageing time and temperature.

In this work, we introduce an innovative approach for measuring K, aiming at avoiding issues related to load line rigidity of the testing machine. It involves confined compression by using a transparent polymethyl methacrylate (PMMA) crucible equiped with optical extensometry to follow the local deformation of the material. The integration of optical extensometry with a transparent PMMA crucible presents some advantages such as, providing enhanced insights into oedometric response analysis and precision in the measurement of the elastomer's bulk modulus. This methodology allowed a better understanding of the material's deformation during the confined compression.

After providing the definition of bulk modulus and discussing the assumption of incompressibility, commonly considered in elastomer studies, the following sections introduce the material under study and the methods used to determine the bulk modulus K. Additionally, an approach to tracking the evolution of K with ageing is outlined.

2. Background

2.1. Incompressibility assumption

Elastomers are commonly assumed to be incompressible, which is generally admitted without any checking. One way to verify this by using tensile/compression tests consists of measuring full field displacement by digital image correlation (DIC) technique. By considering an isotropic material, at least with transversal isotropy, the longitudinal and the transverse elongations λ_L and λ_T can be accessed (Anssari-Benam and Horgan, 2022). In Logeais et al. (2022), we carried out such a checking by using H2 dog bones [ISO 527-2] and discs specimens for, respectively, tensile and compression tests. The aforementioned two elongations were measured by marker tracking, allowing the volume change to be determined all along the test. The jacobian of the transformation $J = \det(\underset{\sim}{F})$, where $\underset{\sim}{F}$ is the deformation gradient, is the ratio between the actual volume V with respect to the initial volume V_0 during the test:

$$J = \frac{V}{V_0} = \lambda_L \times \lambda_T^2 \tag{1}$$

Fig. 1 shows the evolution of J as a function of the longitudinal elongation for both tensile/compression tests, respectively triangle and round points. It is observed that the evolution of J varies with elongation following a non-linear trend. Moreover, the response of J is not the same under tension and compression tests. At the same applied strain rate, the change in volume J seems more critical in the case of a compression test.

Recall that the strict incompressibility assumption should lead to no volume change of the material during the mechanical loading, so that J should remain constant, equal to one. The horizontal red line in Fig. 1 characterises this no-volume change assumption. The deviation from incompressibility assumption, for the fluorosilicone, is clearly highlighted.

Under small strain framework, by using $J - 1 = \Delta V / V_0$ and $\lambda = 1 + \varepsilon$ for both longitudinal and transverse direction, with ε the engineering strain, Eq. (1) becomes:

$$\frac{\Delta V}{V_0} \approx \varepsilon_L + 2\varepsilon_T \tag{2}$$

Taking the isotropy of the material into account, the Poisson's ratio ν is defined as $\nu = -\varepsilon_T / \varepsilon_L$, yielding then (Schwarzl et al., 1967):

$$\frac{\Delta V}{V_0} = \varepsilon_L (1 - 2\nu) \tag{3}$$

As aforementioned, the incompressibility assumption should lead to no volume change, i.e. $\Delta V = 0$, then, from Eq. (3), $\nu = 0.5$.

The Poisson's ratio is related with the bulk modulus and the Young's modulus E by Barney et al. (2022):

$$K = \frac{E}{3(1 - 2\nu)} \tag{4}$$

Furthermore, $\nu = 0.5$ leads to an asymptotic value of K as plotted in Fig. 2. Indeed, a small change on ν near 0.5 can induce significant change in K.

The assumption of incompressibility is an approximation and does not apply perfectly to all types of elastomers and to all loading conditions. Some elastomers can exhibit significant volume changes, often referred to as quasi-incompressibility. In the literature, the bulk modulus plays a critical role in materials subjected to hydrostatic pressure (Zimmermann and Stommel, 2013), laminated rubber (Bouaziz et al., 2020; Hao et al., 2024) or in the context of cavitation failure (Gent and Lindley, 1959; Barney et al., 2020).

In summary, the incompressibility assumption has not been verified for fluorosilicone and monitoring the compressibility over time appears to be critical for sealing applications. The bulk modulus is commonly characterised by measuring E and ν; however, for a quasi-incompressible material, a small uncertainty in its measurement will give a large uncertainty in K (Burns et al., 1990, 1987). This motivates a direct measurement of K so as to better assess the liability of the sealing for a long period.

2.2. The bulk modulus K

The bulk modulus measures a material's resistance to volumetric compression, i.e. the volume change concerning an applied hydrostatic pressure. It is described by the following equation:

$$K = -\frac{V\, dP}{dV} \tag{5}$$

where dP is the pressure variation, V the initial volume, and dV the volume variation. In this equation, a compressive pressure change, where $dP > 0$, will result in a decrease in volume, $dV < 0$. Consequently, this relationship implies that for an isotropic material the bulk modulus K will be greater than zero.

Compared with other elastic moduli such as Young's modulus E and shear modulus G, establishing a relationship between bulk modulus and the internal structure of the elastomer is challenging. This complexity

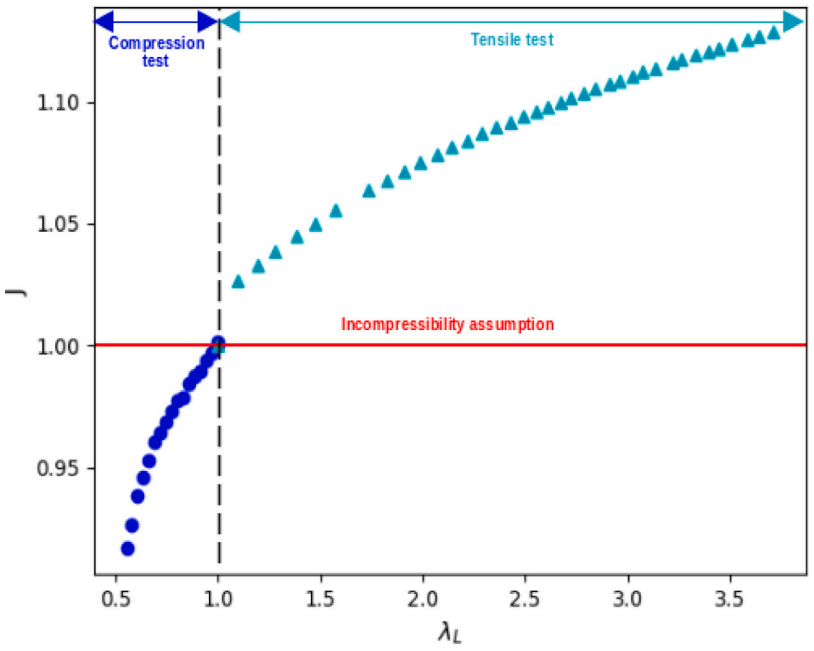

Fig. 1. Jacobian of the transformation J – volume change – as a function of applied strain in uniaxial tension and compression of a FVMQ (Logeais et al., 2022).

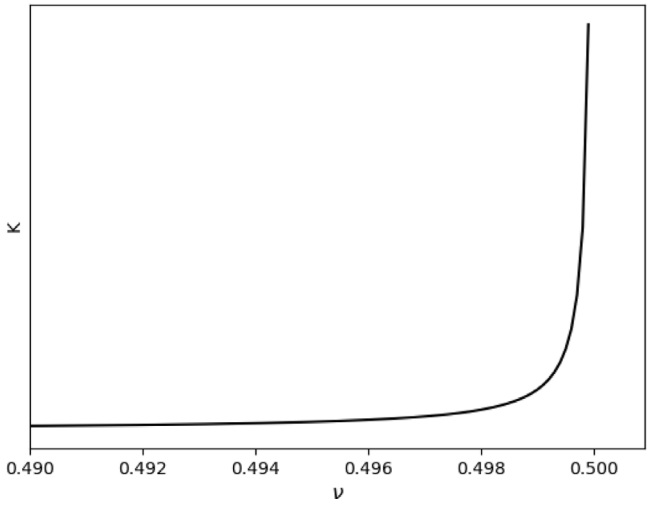

Fig. 2. Evolution of K with as function of ν.

arises as the bulk modulus characterises a volumetric property at macroscopic scale. The main hypothesis often used in the literature to elucidate the mechanism governing the bulk modulus is the one presented by Tabor (1994). According to Tabor's framework, Young's modulus E and bulk modulus K can be attributed to different intermolecular mechanisms. In this conceptualisation, the bulk modulus is attributed to intermolecular forces, specifically van der Waals forces acting between the methylene group and its neighbours.

Theoretically, two elastic material parameters are enough to use Hooke's law in the small strain framework. The calculation of the stress (*resp.* strain) tensor can then be completed when the strain (*resp.* stress) tensor is known. Let us consider here that the strain tensor $\underset{\sim}{\varepsilon}$ is known. Then, the terms of the stress tensor $\underset{\sim}{\sigma}$ read:

$$\sigma_{ij} = \frac{E}{1+\nu}\left(\varepsilon_{ij} + \frac{\nu}{1-2\nu}\varepsilon_m \delta_{ij}\right) \quad (i,j) \in \{1,2,3\} \tag{6}$$

where δ_{ij} is the Kronecker symbol, $\delta_{ij} = 1$ if $(i = j)$ and $\delta_{ij} = 0$ if $(i \neq j)$, and

$$\varepsilon_m = \frac{\text{trace}(\underset{\sim}{\varepsilon})}{3} \tag{7}$$

In the case of confined compression tests (Weir, 1953; Adams and Gibson, 1930; Scott, 1935; Copeland, 1948; Tizard et al., 2012; Stanojevic and Lewis, 1983), in cylindrical coordinates (r, θ, z), z being the loading direction, the strain tensor is known to be uniaxial. Actually, the unique component of the strain tensor is $\varepsilon_z = \frac{\Delta H}{H_0}$, where H_0 and ΔH are respectively the initial height of the specimen, at the onset of the confined compression test, and the contraction of the specimen. Note that ΔH is negative. From Eq. (6), the principal stresses can be determined as follows:

$$\sigma_r = \sigma_\theta = \frac{E}{1+2\nu}\frac{\nu}{1+\nu}\frac{\Delta H}{H_0} \tag{8}$$

$$\sigma_z = \frac{E}{1+2\nu}\frac{1-\nu}{1+\nu}\frac{\Delta H}{H_0} \tag{9}$$

σ_z is, by definition, equal to F/S_0 where F is the load and S_0 is the area of the cross section, which does not change because of the rigid crucible.

Therefore:

$$\sigma_z = \frac{F}{S_0} = \frac{E}{1+\nu}\frac{1-\nu}{1+\nu}\frac{\Delta H}{H_0} \tag{10}$$

Knowing then the slope of the stress–strain curve and the Young's modulus, Eq. (10) leads to a second degree equation on ν. The positive solution for ν can be selected, which enables to calculate K by using Eq. (4) (Barney et al., 2022).

In the following, Eq. (4) was substituted into Eqs. (8) and (9):

$$\sigma_r = \sigma_\theta = 3K\frac{\nu}{1+\nu}\frac{\Delta H}{H_0} \tag{11}$$

$$\sigma_z = 3K\frac{1-\nu}{1+\nu}\frac{\Delta H}{H_0} \tag{12}$$

Table 1
Ageing times for each ageing temperature.

Ageing temperature (°C)	200	220	250
Ageing times (h)	0	0	0
	168	168	24
	336	504	48
	504	840	72
	1512	1176	96
	2520	1680	120
	5712	2520	168

Note that, from Eqs. (11) and (12), when $\nu \to 0.5$ then $1-\nu \approx \nu$. Therefore, in a confined compression test, the stress tensor is equi-triaxial, *i.e.* $\sigma_r = \sigma_\theta = \sigma_z$. Finally, from Eq. (12) the bulk modulus can be derived:

$$K = \frac{1}{3}\frac{1+\nu}{1-\nu}\frac{\frac{F}{S_0}}{\frac{\Delta H}{H_0}} \tag{13}$$

At last, the approximation $\nu \approx 0.5$ leads to the simple result :

$$K \approx \frac{\frac{F}{S_0}}{\frac{\Delta H}{H_0}} \tag{14}$$

meaning that the bulk modulus is the slope of the stress–strain curve in a "real" confined compression test. The experimental challenge is then the determination of the time when the specimen is in the confined state, which is a key point to accurately measure, ΔH and H_0 with respect to F.

3. Material, design and method

3.1. Material and specimen

The study is based on the analysis of a FVMQ elastomer which is a copolymer composed mainly of triofluoropropylsiloxane, dimethylsiloxane and methylvinylsiloxane with 0.75 phr peroxide. The elastomer is filled with silice and titane oxide. It is a modified silicone in which some $-CH_3$ groups are replaced by $-CH_2CH_2CF_3$ in the polymer repeat unit.

The material was supplied by *ITC Élastomères* in the form of 2 mm thick plates. In order to obtain the samples, discs with a diameter of 20 mm were cut-out directly from the plate using a circular punch.

3.2. Ageing of specimens

The in-service ageing process has been mimicked, providing valuable insight into the durability of elastomeric materials, by accelerated ageing. This approach is particularly important for understanding how the compressibility of an elastomer changes over time, as it allows data to be extrapolated beyond the typical duration of laboratory tests.

In the accelerated ageing protocol, sheets were placed in an oven under air at three temperatures: 200, 220 and 250 °C up to 34, 15 weeks and 1 week respectively. After ageing, the samples were prepared in the same way as the pristine specimens, allowing the confined compression tests to be carried out at room temperature. Table 1 shows the ageing times tested for each ageing temperature. Note that 2 samples have been tested for each ageing time and temperature condition.

3.3. Oedometric compression setup

Confined compression tests, also referred to as oedometer compression, were performed on FVMQ discs. This testing method allows for the application of quasi-equitriaxial loading, reproducing similar conditions to those in a sealing application. A disc sample is placed in an oedometer cell, with the primary goal of accurately monitoring the specimen's height variation as the load is applied.

In this work, a new experimental setup is proposed to determine the bulk modulus by measuring the local displacement using a PMMA crucible. Fig. 3 illustrates the experimental setup. Fig. 3(a) shows the system, with the transparent-polymer crucible, the metallic piston and a white specimen. The PMMA crucible consist of a cubic external structure of 40 mm side length, which provides adequate resistance during the oedometric compression tests. The transparency allows following the local elongation of the specimen by using a camera synchronised with the testing machine. The internal shape is cylindrical with an internal diameter of 20 mm with an upper tolerance of 0.045 mm. A metal base is placed at the bottom of the crucible with calibrated points and lines spaced at 1 mm intervals, i.e. a point is followed by a line separated by 0.5 mm. Fig. 3(b) shows an example of an image taken with the camera. This allows a permanent view of the scale during the test used as optical extensometer. To exert a load on the sample inside the crucible, a metallic piston of 19.95 mm diameter is used. This clearance of 25 μm from the internal diameter is a compromise between avoiding friction between the crucible and piston and minimising the extrusion of material in this gap. In addition, some lubricant (here Vaseline) was applied to the surfaces of the metal piston to facilitate its displacement through the crucible.

The tests were performed at room temperature on an Instron testing machine with a 10 kN load cell. A crosshead displacement rate of 0.5 mm/min was applied. The maximum load was limited to 8 kN, to avoid damage of the crucible.

Images were captured using a 4 megapixel camera at 2 images per second. Local displacement was measured by an optical extensometer using the Vicgauge2D software. In fact, it is possible to save images and follow simultaneously the local displacement at different frequencies. Therefore, synchronised with Instron machine data, the local displacement sampling rate is approximately 50 Hz. The virtual point of the optical extensometer is placed on the piston, thanks to the pattern created with speckles, and the calibrated points and lines on the metal base. The displacement measured by the optical extensometer thus represents the local displacement view through the verticales surfaces of the specimen.

The lateral surfaces of the crucible were monitored using a camera all along the test. No visible displacement was reported. Therefore, the lateral deformation of the crucible during the test was considered to be negligible. Note that, using a steel cylinder, Holownia (1975) proposed a methodology to correct this phenomenon if needed.

3.4. Secant/tangent bulk modulus

Once the data have been collected and reduced only to the confined condition, the tangent R_t and secant R_s stiffnesses can be determined analytically as follows:

$$\begin{cases} R_t = \dfrac{\sigma_i - \sigma_{i-1}}{\varepsilon_i - \varepsilon_{i-1}} \\ \\ R_s = \dfrac{\sigma_i - \sigma_0}{\varepsilon_i - \varepsilon_0} \end{cases} \tag{15}$$

As mentioned in Section 2.2, for $\nu \approx 0.5$, the K_t and K_s can be considered equal to R_t and R_s respectively. In other mechanical tests, the secant modulus is often used to characterise the initial stiffness of an elastic material, K_s is then a measure in the elastic region of the material. It is an average of the slope of a linear stress–strain curve, up

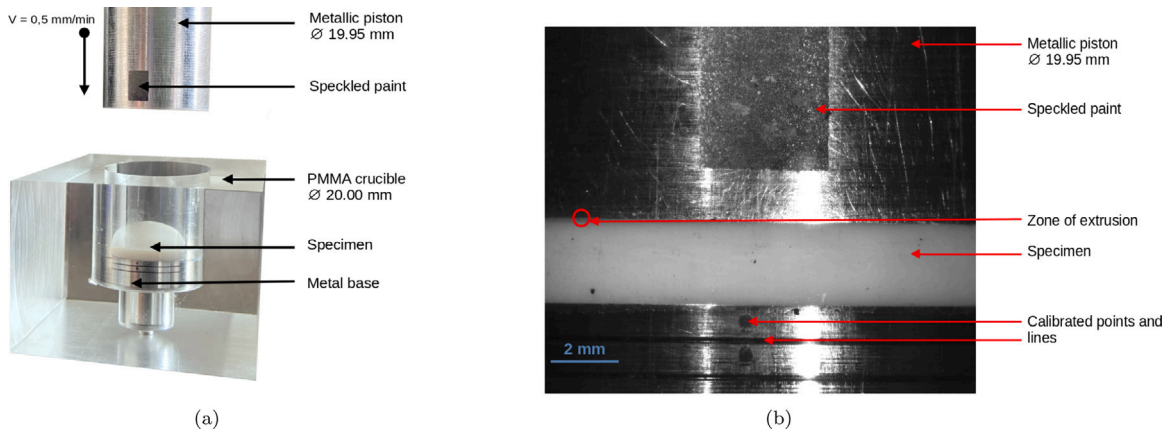

Fig. 3. Oedometric compression device in PMMA: (a) Oedometric set-up; (b) acquisition image.

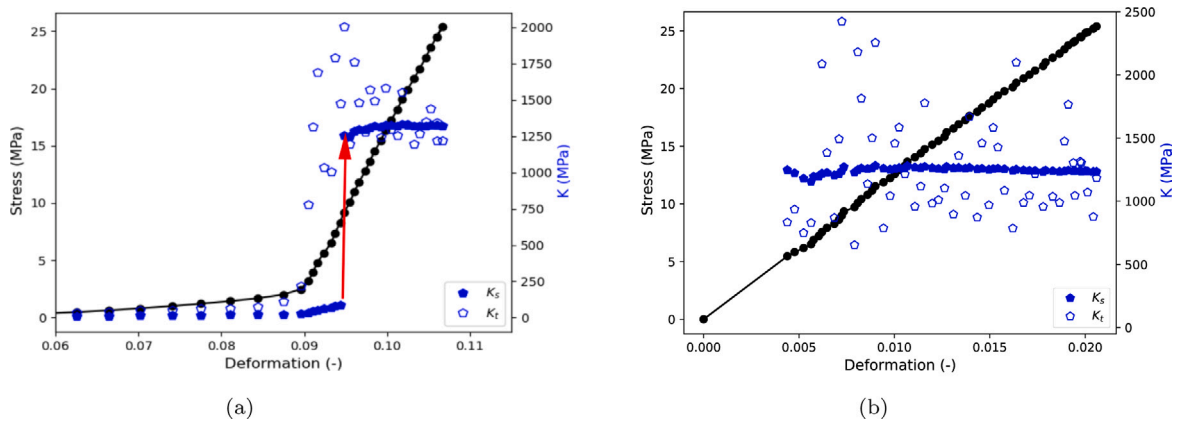

Fig. 4. Stress–strain curve for confined compression, illustrating the difference between the secant and tangent bulk modulus before (a) and after (b) correction of the "toe region".

to the deviation from linearity. The K_t is a measure of the ratio of stress to strain at a given point on the stress–strain curve. It is calculated from the instantaneous slope of the curve at a given point. It can be used to characterise the elastic behaviour of the material at a given level of deformation. If the stress–strain curve is linear, then $K_s = K_t$

In the case of the oedometric compression test, the aim is to obtain the value of the bulk modulus on the linear part. The equivalence between K_s and K_t is only obtained if the "toe region" is removed from the data exploited.

Fig. 4 presents the stress–strain curves (black curves) obtained from confined compression tests, displayed before (Fig. 4(a)) and after dimension correction (Fig. 4(b)). The secant and tangent moduli are represented by light and dark blue hexagonal symbols, respectively.

After applying this correction and determining the bulk modulus by Eq. (15), Fig. 4(b) is obtained. It can be observed that K_t is much scattered, but its average value seems to fit with K_s once the initial point (σ_0, ϵ_0) is correctly determined.

4. Results and discussions

4.1. Response at the unaged state

This section presents the oedometer compression results on the fluorosilicone elastomer using the experimental set-up and methodology presented previously. This integrated approach not only allows real-time observation of the specimen response, but also provides critical information for post-processing of the data, enhancing the overall analysis of the oedometer compression test results.

Fig. 5 provides a visual representation of the compression oedometer test results. In Fig. 5(a), the blue line shows the local displacement (Δh) of the fluorosilicone elastomer with respect to the crosshead displacement imposed by the tensile machine shown by the black solid line (ΔH). The green line shows the evolution of the load as a function of the displacement. Four specific points are marked on the local displacement curve for clarity and ease of the interpretation. Corresponding images capturing the state of the specimen at these marked points during the test are shown on Fig. 5(b). This dual presentation allows a combination of the quantitative data (displacement and force) and the qualitative visual observations of the deformed system.

- Point ①: represents the beginning of the test, when the specimen is placed in the crucible and the piston comes into first contact with it. At this point no load or displacement is imposed on the material, but it can be seen that a gap exists between the specimen and the piston due to a non-planarity of the top surface. Inaccuracies in the alignment of the test system or non-planar contact surfaces can result in unequal loading and deformation across the specimen. This lack of uniformity can affect the reliability and repeatability of test results. At this point, the oedometric conditions are not satisfied because the specimen is not fully confined inside the crucible. Furthermore, up to a displacement of 0.1 mm, it can be seen that the optical displacement follows the imposed crosshead displacement.
- Point ②: after 0.1 mm of displacement, the local displacement curve falls away from the imposed displacement and load increases non-linearly. The local displacement on the specimen is lower than the crosshead one. Looking at the corresponding image on the point ②, it can be seen that the colour of the specimen appears darker compared with the first image. This is due to the contact between the sample and the wall of the crucible. It has

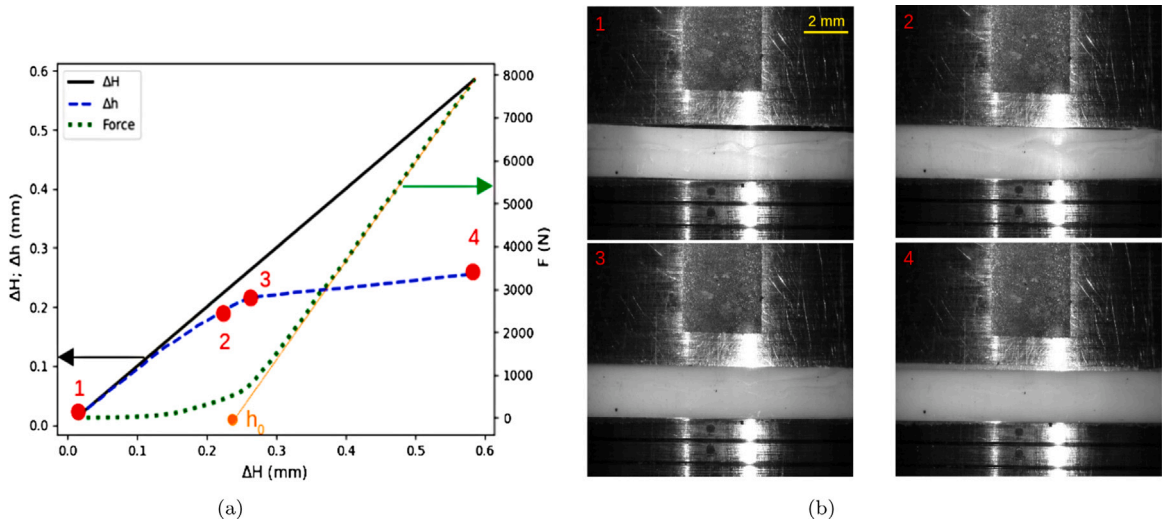

Fig. 5. Oedometric compression test on fluorosilicone: (a) Load vs. displacement curve; (b) Images showing the deformed state in the crucible at each step in (a). (For interpretation of the references to colour in this figure legend, the reader is referred to the web version of this article.)

filled the empty space left in the set up. However, the oedometric state is not yet stable because there is still a gap between the sample and the piston and the sample is not completely stacked on the crucible.

- Point ③: there is an inflection of the local displacement and the force. The corresponding image shows that the material is completely confined in this state, so the oedometric condition is verified. From this point, initial h_0 and s_0 were measured so as to obtain the bulk modulus which can be determined all along the linear part, up to point ④.
- Point ④: slight extrusion of the material is observed at the top of the specimen. As linearity is maintained throughout the test up to 8 kN, the extrusion effect can be considered as negligible.

These results suggest that the non-linear part at the beginning of the test corresponds to the sample settling within the measurement system. Additionally, the inflection point in the force–displacement curve corresponds to the moment when the material is fully confined within the crucible. The new initial height could be determined by the projection of the curve until the intersection with the abscissa, as shown in Fig. 5(a) at the h_0 point. For a better understanding of how to correct the characteristic dimensions of the specimen for stress and strain calculations, the reader can refer to Appendix.

The method outlined in Section 3.4 and on the Appendix will therefore be used for the post-processing of the results. The bulk modulus of the FVMQ was determined by performing two tests on unaged specimens. The bulk modulus determined was 1310±23 MPa, consistent with values found in the literature (Bouaziz et al., 2020; Barney et al., 2022). The bulk modulus is high enough to consider this material for sealing applications.

In summary, using a transparent crucible made of PMMA for confined compression tests on elastomers offers one significant advantage dealing with the real-time visualisation of the material's deformation during the test. Namely, this allowed a better understanding of the large "toe" region at the beginning of the stress–strain curve. Additionally, local displacement measurements can be obtained, overcoming potential issues encountered in blind tests, such as those using metal crucibles. However, the main drawback concerns the accuracy of the measurement. Regarding the use of optical extensometer, the use of a higher resolution camera could improve accuracy due to the very small deformation observed on the specimen. Also, measurements are limited to the surface of the specimen visible to the camera, which can lead to uncertainties due to loadline or material heterogeneity. These factors should be carefully considered when using transparent crucibles for confined compression testing.

The next step consists of characterisation of the evolution of K with ageing to ensure that the sealing function is maintained throughout the service life of the engineering structure.

4.2. Evolution of K with ageing

After accelerated thermo-oxidative ageing on FVMQ plates at 200, 220 and 250 °C up to 34, 15 and 1 weeks respectively, the samples were tested using the same PMMA crucible. For each time/temperature pair selected, the material was tested twice to ensure reproducibility of the results.

At 250 °C, in order to ensure material integrity, the ageing time was limited to 1 week. Indeed, beyond this time, the material will be completely degraded and brittle. Delamination occurred on both edges of the specimen. For ageing at 200 and 220 °C, the integrity of the material was observed at the maximal ageing times, respectively 34 and 15 weeks, the ageing time could then be extended.

Fig. 6 shows the evolution of K with ageing time parameterised by the ageing temperature. For the sake of clarity, Fig. 6 is presented with a semi-logarithmic scale due to the large range of ageing times. This scale allows all temperatures to be displayed on the same graph. The evolution of K is normalised by the bulk ratio K/K_0 recalling that K_0 is the bulk modulus at the unaged state equal to 1310±23 MPa. Due to the semi-logarithmic scale, the bulk ratio cannot be plotted at t = 0 h. Therefore, the unaged bulk ratio is reported to 10^0 h. The red, blue and green dashed lines represent ageing temperatures of 250, 220 and 200 °C, respectively.

A "linear" decrease of the bulk ratio is followed by a steeper one at 1512 h, 840 h and 24 h at 200, 220 and 250 °C respectively. The evolution appears to be similar but with slower kinetics at lower temperatures. This implies that the degradation mechanisms responsible for the decrease in K for FVMQ accelerate at higher ageing temperatures.

The evolution of K at 250 °C undergoes a significant decrease, losing approximately 30% of its initial value, after 72 h of ageing. Beyond this ageing period, the modulus increases until it reaches a value corresponding to a loss of approximately 20% of the initial bulk modulus. After one week, as aforementioned, the material undergoes significant degradation, rendering it unsuitable for further testing.

Besides, the bulk modulus K exhibits a gradual decrease of approximately 40% and 30% after 15 weeks at 220 °C and 200 °C, respectively. For these ageing times, there is no increase in K as observed at 250 °C.

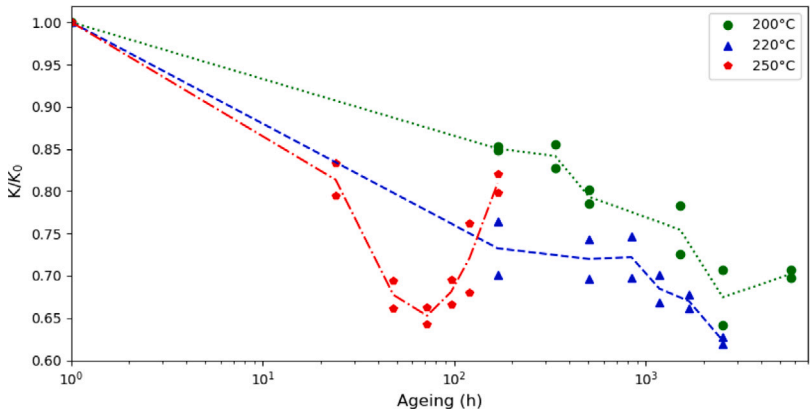

Fig. 6. Influence of ageing on K of FVMQ at 200, 220 and 250 °C with $K_0 = 1300$ MPa. (For interpretation of the references to colour in this figure legend, the reader is referred to the web version of this article.)

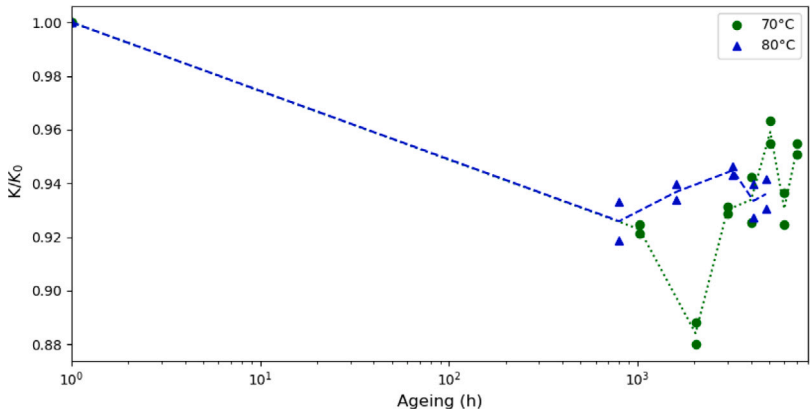

Fig. 7. Influence of ageing on K of polychloroprene at 70, 80 °C with $K_0 = 1100$ MPa (Bouaziz et al., 2020). (For interpretation of the references to colour in this figure legend, the reader is referred to the web version of this article.)

It is expected that for lower ageing temperatures, the same profile as at 250 °C should be found, but the minimum K should be shifted to a longer period. Ageing at 200 °C was extended to 34 weeks. K appears to stabilise between the two last ageing times. This highlights the complex relationship between ageing temperature and time, which influences the compressibility characteristics of the material over time.

Fig. 7 presents the results of the evolution of K with ageing for a polychloroprene – using a metallic crucible – in the study of Bouaziz et al. (2020). The same semi-log representation of the ageing time and evolution of K is used in this graph. The blue and green dashed lines represent ageing temperatures of 80, 70 °C, respectively. A "linear" decrease is observed for both ageing temperatures until 1025 and 800 h for 70 and 80 °C.

At 80 °C, the evolution of K seems to be stabilised. At 70 °C, in line with our observations, the initial decrease was followed by a steeper one up to 2032 h. In agreement with FVMQ at 250 °C, the steeper decrease was followed by a bulk modulus increase. This was followed by a stabilisation of K with a loss of about 5% at the end of the ageing. Assuming that a high temperature increases the kinetics of the mechanisms responsible for the evolution of K, similar phenomenon is supposed to occur at 80 °C with a lower ageing time, which has not been tested. The trend seems to be similar to the FVMQ results. However, the decrease in K seems to be less significant than on the FVMQ.

These results indicate that compressibility varies with time and that there are two distinct ageing states. Taking the example of ageing at 250 °C, several hypotheses can be proposed to explain the evolution of K over time. The degradation of the polymer matrix, which could lead to porosity in the material, appears to be the most plausible explanation for the first part of the curve. The presence of voids would likely decrease the bulk modulus. Subsequently, as noted, the material stiffens and undergoes embrittlement after 72 h of ageing. This change in the elastomer could be attributed to ageing mechanisms such as chain-scission and post-crosslinking, which may explain the observed increase in bulk modulus after 72 h. This phenomenon may have a detrimental impact on the component's ability to deform and conform to contact surfaces where it is confined, potentially increasing the risk of leakage in sealing applications. Although the bulk modulus increases again, this zone appears to be avoided when using the material in an engineering structure due to these factors. These various results highlight that the bulk modulus value must be considered alongside other end-of-life criteria.

5. Conclusions

In this work, the compressibility of fluorosilicone elastomer (FVMQ) used for sealing application was explored. The incompressibility assumption for elastomers was questioned and it was suggested that it should be verified through a uniaxial test, measuring longitudinal and transverse strain, by considering an isotropic material. For FVMQ, this assumption is not verified in either compression or tensile tests. In the case of O-ring components, the bulk modulus K must be controlled to ensure a correct sealing over a long service life. In this study, a confined compression test with a transparent crucible has been used to follow the local displacement with an optical extensometer. Transparency allows the oedometric compression data to be understood, resulting in a more accurate measure used to calculate the bulk modulus. As a matter of fact, this method provided a reliable K value of 1310 MPa,

sufficient for sealing applications. In the second part, the evolution of K over time was studied by applying accelerated ageing, using the same experimental set-up. Three temperatures – 200, 220 and 250 °C – were tested and showed a decrease in K over time with kinetics more significant at high temperature. At 250 °C, an increase was observed after 72 h of ageing. These results were similar to those found in the limited report in the literature on the subject and showed that the sealing of an engineering system can be compromised after a certain period of operation.

Although the time-dependent response of the compressibility modulus was not studied in this work, their impact on seal performance is worthy of further investigation. Future work should focus on the time-dependent response of the bulk modulus, as stress relaxation is a critical factor that can significantly influence the mechanical response of the material under long-term confined compression.

CRediT authorship contribution statement

Clémence Logeais: Writing – review & editing, Writing – original draft, Visualizsation, Methodology, Investigation, Conceptualization. **Cristian Ovalle:** Writing – review & editing, Validation, Supervision, Methodology, Conceptualization. **Lucien Laiarinandrasana:** Writing – review & editing, Validation, Supervision, Methodology, Conceptualization.

Declaration of competing interest

The authors declare that they have no known competing financial interests or personal relationships that could have appeared to influence the work reported in this paper.

Acknowledgements

The authors would like to thank “ITC Élastomères” for providing the material, as well as the ANR, the French National Research Agency, for supporting this project (ANR-20-CE06-0024). Special thanks are also extended to the members of the laboratory, particularly the SESAMES platform, especially Jean-Christophe TEISSEDRE, and the members of the AT JPE platform, for their invaluable help and support throughout this work. Their technical expertise and dedication greatly contributed to the success of this study.

Appendix. Determination of K: characteristic dimensions

The method presented here is based on qualitative analyses of the confined compression test. The results are presented in detail in 4.1.

In the case of an oedometer test, the engineering stress and strain are considered equivalent to the true stress and strain due to the transverse confinement, as the cross section remains constant throughout the test. For this reason, engineering stress and strain are used to calculate the bulk modulus K. As mentioned before, the bulk modulus is calculated from the stiffness obtained in the linear part of the stress–strain curve. Commonly, in confined compression tests, the initial dimensions of the specimen, as measured by a caliper gauge, are taken into account in:

$$\begin{cases} \sigma = \dfrac{F}{S_0} \\ \varepsilon = \dfrac{\Delta H}{H_0} \end{cases} \tag{A.1}$$

where F is the force applied, S_0 the initial section, ΔH the imposed displacement and H_0 the inital thickness of the specimen. However, corrections must be applied to these initial dimensions. Actually, the dimensions used for calculation should correspond to those when the material is fully confined in the crucible.

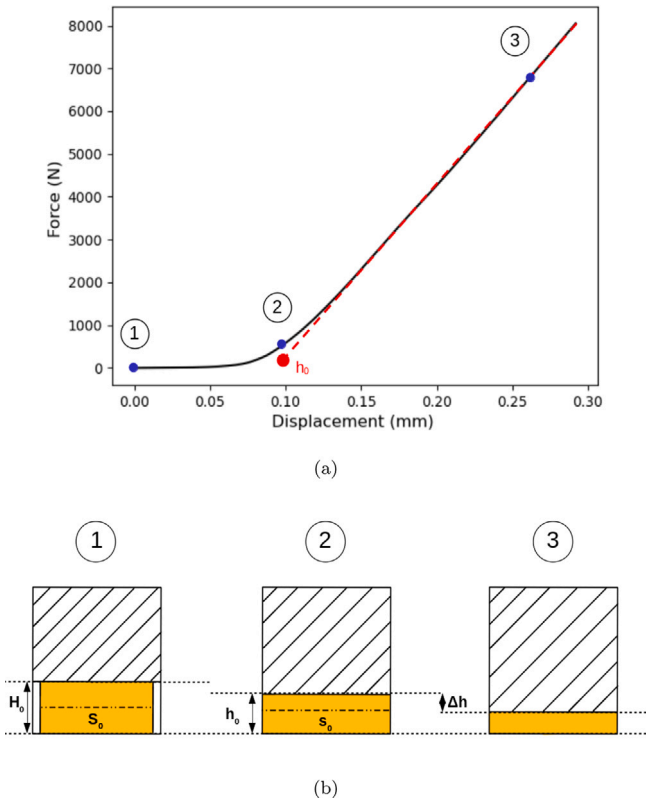

Fig. A.8. Correction of dimensions and determination of K: (a) Load vs. displacement curve; (b) Deformed shapes of the specimen inside the crucible.

Fig. A.8(a) shows the force applied as a function of applied crosshead displacement. Three characteristic events labelled ①, ②and ③points are marked inside the graph. Fig. A.8(b) illustrates the deformed shapes of the sample corresponding to the 3 events.

At the start of the test (label ①), the sample is placed in the crucible and the piston is in contact with the top surface of the sample. The side surface of the sample is not perfectly bonded to the internal wall of the crucible. The material is not completely enclosed, the oedometric conditions are not fully satisfied. Between ①and ②, the loading is assumed to be uniaxial until the specimen is fully confined in the system. After a displacement ΔH_0, inflection point marked by label ②, the force increases linearly, e.g. curve segment between ②and ③. Indeed, it corresponds to the moment when the specimen is completely confined within the oedometric system. Consequently, the specimen has a new cross-section corresponding to the internal diameter of the crucible noted as s_0. The new initial height, $h_0 = H_0 - \Delta H_0$, could be determined by the projection of the curve until the intersection with the abscissa, as shown in Fig. A.8(a). So the new expression of stress and strain is defined as:

$$\begin{cases} \sigma = \dfrac{F}{s_0} \\ \varepsilon = \dfrac{\Delta h}{h_0} \end{cases} \tag{A.2}$$

This setting allows the behaviour of the material under the specific conditions of the oedometric test to be accurately determined. Thanks to the transparent crucible, optical extensometer could be used to measure these key lengths.

Data availability

Data will be made available on request.

References

Adams, L.H., Gibson, R.E., 1930. The compressibility of rubber. J. Wash. Acad. Sci. 20 (12), 213–223, URL https://www.jstor.org/stable/24529237. Publisher: Washington Academy of Sciences.

Anssari-Benam, A., Horgan, C.O., 2022. New constitutive models for the finite deformation of isotropic compressible elastomers. Mech. Mater. 104403. http://dx.doi.org/10.1016/j.mechmat.2022.104403, URL https://linkinghub.elsevier.com/retrieve/pii/S0167663622001739.

Barney, C.W., Dougan, C.E., McLeod, K.R., Kazemi-Moridani, A., Zheng, Y., Ye, Z., Tiwari, S., Sacligil, I., Riggleman, R.A., Cai, S., Lee, J.-H., Peyton, S.R., Tew, G.N., Crosby, A.J., 2020. Cavitation in soft matter. Proc. Natl. Acad. Sci. 117 (17), 9157–9165. http://dx.doi.org/10.1073/pnas.1920168117, URL https://pnas.org/doi/full/10.1073/pnas.1920168117.

Barney, C.W., Helgeson, M.E., Valentine, M.T., 2022. Network structure influences bulk modulus of nearly incompressible filled silicone elastomers. Extreme Mech. Lett. 52, 101616. http://dx.doi.org/10.1016/j.eml.2022.101616, URL https://linkinghub.elsevier.com/retrieve/pii/S2352431622000074.

Bernstein, R., Gillen, K., 2009. Predicting the lifetime of fluorosilicone o-rings. Polym. Degrad. Stab. 94 (12), 2107–2113. http://dx.doi.org/10.1016/j.polymdegradstab.2009.10.005, URL https://linkinghub.elsevier.com/retrieve/pii/S0141391009003309.

Bhuvaneswari, C.M., Kale, S.S., Gouda, G., Jayapal, P., Tamilmani, K., 2017. Elastomers and adhesives for aerospace applications. In: Prasad, N.E., Wanhill, R.J.H. (Eds.), Aerospace Materials and Material Technologies. Springer Singapore, pp. 563–586. http://dx.doi.org/10.1007/978-981-10-2134-3-26, URL http://link.springer.com/10.1007/978-981-10-2134-3-26. series Title: Indian Institute of Metals Series.

Bouaziz, R., Truffault, L., Borisov, R., Ovalle, C., Laiarinandrasana, L., Miquelard-Garnier, G., Fayolle, B., 2020. Elastic properties of polychloroprene rubbers in tension and compression during ageing. Polymers 12 (10), 2354. http://dx.doi.org/10.3390/polym12102354, URL https://www.mdpi.com/2073-4360/12/10/2354.

Burns, J., Dubbelday, P.S., Ting, R.Y., 1987. Bulk modulus of elasticity of various elastomers: theory and experiment. 39.

Burns, J., Dubbelday, P.S., Ting, R.Y., 1990. Dynamic bulk modulus of various elastomers. Journal of Polymer Science Part B: Polymer Physics 28 (7), 1187–1205. http://dx.doi.org/10.1002/polb.1990.090280715, URL https://onlinelibrary.wiley.com/doi/10.1002/polb.1990.090280715.

Camino, G., Lomakin, S., Lazzari, M., 2001. Polydimethylsiloxane thermal degradation part 1. kinetic aspects. Polymer 42 (6), 2395–2402. http://dx.doi.org/10.1016/S0032-3861(00)00652-2, URL https://linkinghub.elsevier.com/retrieve/pii/S0032386100006522.

Cassenti, B.N., Staroselsky, A., 2017. Deformation and stability of compressible rubber O-rings. Int. J. Mech. Mater. Eng. 12 (1), 5. http://dx.doi.org/10.1186/s40712-017-0072-8, URL http://link.springer.com/10.1186/s40712-017-0072-8.

Copeland, L.E., 1948. The thermodynamics of a strained elastomer. II. compressibility. J. Appl. Phys. 19 (5), 445–449. http://dx.doi.org/10.1063/1.1698153, URL https://pubs.aip.org/jap/article/19/5/445/158987/The-Thermodynamics-of-a-Strained-Elastomer-II.

Cox, J.M., Wright, B.A., Wright, W.W., 1964a. Thermal degradation of fluorine-containing polymers. part i. degradation in vacuum. J. Appl. Polym. Sci. 8 (6), 2935–2950. http://dx.doi.org/10.1002/app.1964.070080636, URL https://onlinelibrary.wiley.com/doi/10.1002/app.1964.070080636.

Cox, J.M., Wright, B.A., Wright, W.W., 1964b. Thermal degradation of fluorine-containing polymers. PART II. degradation in oxygen. J. Appl. Polym. Sci. 8 (6), 2951–2961. http://dx.doi.org/10.1002/app.1964.070080637, URL https://onlinelibrary.wiley.com/doi/10.1002/app.1964.070080637.

Diani, J., Fayolle, B., Gilormini, P., 2008. Study on the temperature dependence of the bulk modulus of polyisoprene by molecular dynamics simulations. Mol. Simul. 34 (10–15), 1143–1148. http://dx.doi.org/10.1080/08927020801993388, URL https://www.tandfonline.com/doi/full/10.1080/08927020801993388.

Farfán-Cabrera, L.I., Pascual-Francisco, J.B., Barragán-Pérez, O., Gallardo-Hernández, E.A., Susarrey-Huerta, O., 2017. Determination of creep compliance, recovery and Poisson's ratio of elastomers by means of digital image correlation (DIC). Polym. Test. 59, 245–252. http://dx.doi.org/10.1016/j.polymertesting.2017.02.010, URL https://www.sciencedirect.com/science/article/pii/S0142941816311916.

Farris, R.J., 1964. Dilatation of granular filled elastomers under high rates of strain. J. Appl. Polym. Sci. 8 (1), 25–35. http://dx.doi.org/10.1002/app.1964.070080102, URL https://onlinelibrary.wiley.com/doi/10.1002/app.1964.070080102.

Gent, A.N., Lindley, P.B., 1959. Internal rupture of bonded rubber cylinders in tension. Proceedings of the Royal Society of London. Series A. Mathematical and Physical Sciences 249 (1257), 195–205. http://dx.doi.org/10.1098/rspa.1959.0016, URL https://royalsocietypublishing.org/doi/10.1098/rspa.1959.0016.

Green, H., 1921. Volume increase of compounded rubber under strain. J. Ind. Eng. Chem. 13 (11), 1029–1031. http://dx.doi.org/10.1021/ie50143a033, URL https://pubs.acs.org/doi/abs/10.1021/ie50143a033.

Hao, S., Huang, R., Rodin, G.J., 2024. Constitutive models for confined elastomeric layers: Effects of nonlinearity and compressibility. Mech. Mater. 190, 104912. http://dx.doi.org/10.1016/j.mechmat.2024.104912, URL https://www.sciencedirect.com/science/article/pii/S0167663624000048.

Holownia, B.P., 1975. Effect of carbon black on Poisson's ratio of elastomers. Rubber Chem. Technol. 48 (2), 246–253. http://dx.doi.org/10.5254/1.3547450.

Kalfayan, S.H., Silver, R.H., Mazzeo, A.A., 1975. Accelerated heat-aging studies on fluorosilicone rubber. Rubber Chem. Technol. 48 (5), 944–952. http://dx.doi.org/10.5254/1.3539698, URL https://meridian.allenpress.com/rct/article/48/5/944/90840/Accelerated-HeatAging-Studies-on-Fluorosilicone.

Kelly, J., Lai, J.-W., 2011. The use of tests on high-shape-factor bearings to estimate the bulk modulus of natural rubber. Seismic Isolation and Protective Systems 2 (1), 21–33. http://dx.doi.org/10.2140/siaps.2011.2.21, URL http://msp.org/siaps/2011/2-1/p03.xhtml.

Kömmling, A., Jaunich, M., Pourmand, P., Wolff, D., Gedde, U.W., 2017. Influence of ageing on sealability of elastomeric O-rings. Macromol. Symp. 373 (1), 1600157. http://dx.doi.org/10.1002/masy.201600157, URL https://onlinelibrary.wiley.com/doi/abs/10.1002/masy.201600157.

Laufer, Z., Diamant, Y., Gill, M., Fortuna, G., 1978. A simple dilatometric method for determining Poisson's ratio of nearly incompressible elastomers. Int. J. Polym. Mater. Polym. Biomater. 6 (3–4), 159–174. http://dx.doi.org/10.1080/00914037808077906, URL http://www.tandfonline.com/doi/abs/10.1080/00914037808077906.

Logeais, C., Ovalle, C., Laiarinandrasana, L., 2022. Influence of the compressibility on the mechanical response of a fluorosilicone material. In: Constitutive Models for Rubber XII, first ed. CRC Press, London, pp. 205–210. http://dx.doi.org/10.1201/9781003310266-35, URL https://www.taylorfrancis.com/books/9781003310266/chapters/10.1201/9781003310266-35.

Pires, L., Richaud, E., Roland, S., 2022. Thermal aging of a fluorosilicone rubber. Constitutive Models for Rubber XII-, CRC Press, pp. 415–419. http://dx.doi.org/10.1201/9781003310266-68, Publication title: Constitutive Models for Rubber XII.

Pritchard, R.H., Lava, P., Debruyne, D., Terentjev, E.M., 2013. Precise determination of the Poisson ratio in soft materials with 2D digital image correlation. Soft Matter 9 (26), 6037–6045. http://dx.doi.org/10.1039/C3SM50901J, URL https://pubs.rsc.org/en/content/articlelanding/2013/sm/c3sm50901j. Publisher: The Royal Society of Chemistry.

Ren, W., McMullan, P.J., Griffin, A.C., 2008. Poisson's ratio of monodomain liquid crystalline elastomers. Macromol. Chem. Phys. 209 (18), 1896–1899. http://dx.doi.org/10.1002/macp.200800265, URL https://onlinelibrary.wiley.com/doi/10.1002/macp.200800265.

Schwarzl, F., Bree, H., Nederveen, C., Struik, L., Van Der Wal, C., 1967. On mechanical properties of unfilled and filled elastomers. In: Mechanics and Chemistry of Solid Propellants. Elsevier, pp. 503–538. http://dx.doi.org/10.1016/B978-1-4831-9837-8.50027-2, URL https://linkinghub.elsevier.com/retrieve/pii/B9781483198378500272.

Scott, A., 1935. Specific volume, compressibility, and volume thermal expansivity of rubber-sulphur compounds. J. Res. Natl. Bur. Stand. 14 (2), 99. http://dx.doi.org/10.6028/jres.014.051, URL https://nvlpubs.nist.gov/nistpubs/jres/14/jresv14n2p99_A1b.pdf.

Shuttleworth, R., 1968. Volume change measurements in the study of rubber-filler interactions. Eur. Polym. J. 4 (1), 31–38. http://dx.doi.org/10.1016/0014-3057(68)90005-0, URL https://linkinghub.elsevier.com/retrieve/pii/0014305768900050.

Smith, J.C., Kermish, G.A., Fenstermaker, C.A., 1972. Separation of filler particles from the matrix in a particulate-loaded composite subjected to tensile stress. J. Adhes. 4 (2), 109–122. http://dx.doi.org/10.1080/00218467208072216, URL http://www.tandfonline.com/doi/full/10.1080/00218467208072216.

Stanojevic, M., Lewis, G., 1983. A comparison of two test methods for determining elastomer physical properties. Polym. Test. 3 (3), 183–195. http://dx.doi.org/10.1016/0142-9418(83)90004-1, URL https://linkinghub.elsevier.com/retrieve/pii/0142941883900041.

Tabor, D., 1994. The bulk modulus of rubber. Polymer 35 (13), 2759–2763. http://dx.doi.org/10.1016/0032-3861(94)90304-2, URL https://linkinghub.elsevier.com/retrieve/pii/0032386194903042.

Thomas, D., 1972. High temperature stability in fluorosilicone vulcanisates. Polymer 13 (10), 479–484. http://dx.doi.org/10.1016/0032-3861(72)90087-0, URL https://linkinghub.elsevier.com/retrieve/pii/0032386172900870.

Tizard, G.A., Dillard, D.A., Norris, A.W., Shephard, N., 2012. Development of a high precision method to characterize Poisson's ratios of encapsulant gels using a flat disk configuration. Exp. Mech. 52 (9), 1397–1405. http://dx.doi.org/10.1007/s11340-011-9589-6, URL https://doi.org/10.1007/s11340-011-9589-6.

Van Engelen, N.C., Kelly, J.M., 2015. Correcting for the influence of bulk compressibility on the design properties of elastomeric bearings. J. Eng. Mech. 141 (6), 04014170. http://dx.doi.org/10.1061/(ASCE)EM.1943-7889.0000891, URL https://ascelibrary.org/doi/10.1061/%28ASCE%29EM.1943-7889.0000891.

Weir, C., 1953. Temperature dependence of compression of natural rubber-sulfur vulcanizates of high sulfur content. J. Res. Natl. Bur. Stand. 50 (3), 153. http://dx.doi.org/10.6028/jres.050.024, URL https://nvlpubs.nist.gov/nistpubs/jres/50/jresv50n3p153_A1b.pdf.

Xu, Y.-X., Juang, J.-Y., 2021. Measurement of nonlinear Poisson's ratio of thermoplastic polyurethanes under cyclic softening using 2D digital image correlation. Polymers 13 (9), 1498. http://dx.doi.org/10.3390/polym13091498, URL https://www.mdpi.com/2073-4360/13/9/1498. Number: 9 Publisher: Multidisciplinary Digital Publishing Institute.

Zimmermann, J., Stommel, M., 2013. The mechanical behaviour of rubber under hydrostatic compression and the effect on the results of finite element analyses. Arch. Appl. Mech. 83 (2), 293–302. http://dx.doi.org/10.1007/s00419-012-0655-z, URL http://link.springer.com/10.1007/s00419-012-0655-z.